Electronic Supplementary Material (ESI) for Chemical Communications

Supporting information for the article:

Proton-Electron Transfer Pathways in the Reactions of Peroxyl and dpph• Radicals with Hydrogen-Bonded Phenols

Riccardo Amorati,* Stefano Menichetti, Caterina Viglianisi, Mario C. Foti*

Full text for reference 13:

Gaussian 03, Revision C.02, M. J. Frisch, G. W. Trucks, H. B. Schlegel, G. E. Scuseria, M. A. Robb, J. R. Cheeseman, J. A. Montgomery, Jr., T. Vreven, K. N. Kudin, J. C. Burant, J. M. Millam, S. S. Iyengar, J. Tomasi, V. Barone, B. Mennucci, M. Cossi, G. Scalmani, N. Rega, G. A. Petersson, H. Nakatsuji, M. Hada, M. Ehara, K. Toyota, R. Fukuda, J. Hasegawa, M. Ishida, T. Nakajima, Y. Honda, O. Kitao, H. Nakai, M. Klene, X. Li, J. E. Knox, H. P. Hratchian, J. B. Cross, V. Bakken, C. Adamo, J. Jaramillo, R. Gomperts, R. E. Stratmann, O. Yazyev, A. J. Austin, R. Cammi, C. Pomelli, J. W. Ochterski, P. Y. Ayala, K. Morokuma, G. A. Voth, P. Salvador, J. J. Dannenberg, V. G. Zakrzewski, S. Dapprich, A. D. Daniels, M. C. Strain, O. Farkas, D. K. Malick, A. D. Rabuck, K. Raghavachari, J. B. Foresman, J. V. Ortiz, Q. Cui, A. G. Baboul, S. Clifford, J. Cioslowski, B. B. Stefanov, G. Liu, A. Liashenko, P. Piskorz, I. Komaromi, R. L. Martin, D. J. Fox, T. Keith, M. A. Al-Laham, C. Y. Peng, A. Nanayakkara, M. Challacombe, P. M. W. Gill, B. Johnson, W. Chen, M. W. Wong, C. Gonzalez, and J. A. Pople, Gaussian, Inc., Wallingford CT, 2004.

Homogenous Phase Autoxidations.

Solvents of the highest purity grade were used as received. Styrene was percolated on alumina before each experiment to remove traces of inhibitor. Azobis(isobutyronitrile) (AIBN) was recrystallized from methanol. Kinetic measurements with peroxyl radicals were performed by studying the inhibited autoxidation of styrene or cumene in chlorobenzene or acetonitrile at 303 K, initiated by AIBN (0.05 M), in the presence of variable amounts (2-10 x 10^{-6}M) of the investigated compounds**,** or the synthetic analogue of α-tocopherol 2,2,5,7,8-pentamethyl-6-chromanol (PMHC) as reference antioxidants. The autoxidation was followed by monitoring the oxygen consumption (see Figure S1) in an oxygen uptake apparatus built in our laboratory and based on a Validyne DP15 differential pressure transducer. The rate of initiation R_i was measured in a preliminary set of experiments from the length of the inhibition period T_{inh}, using PMHC as a reference antioxidant: R_i = 2 [PMHC] / T_{inh}. Integration of the oxygen consumption trace afforded the rate of reaction with peroxyl radicals k_{inh}, according to the equation $.\Delta[O_2]_t = -k_p/k_{inh}$ [RH] ln(1-t/ T_{inh}). The k_p values of styrene and cumene at 303° are 41and 0.32 $M^{-1}s^{-1}$ respectively.

In the case of **5**, which showed very poor chain-breaking activity, the k_{inh} value was estimated from the slope of the oxygen consumption, as explained in:

R. Amorati, G. F. Pedulli, L. Valgimigli, O. A. Attanasi, P. Filippone, C. Fiorucci, R. Saladino, *J. Chem. Soc., Perkin Trans. 2*, **2001**, 2142–2146

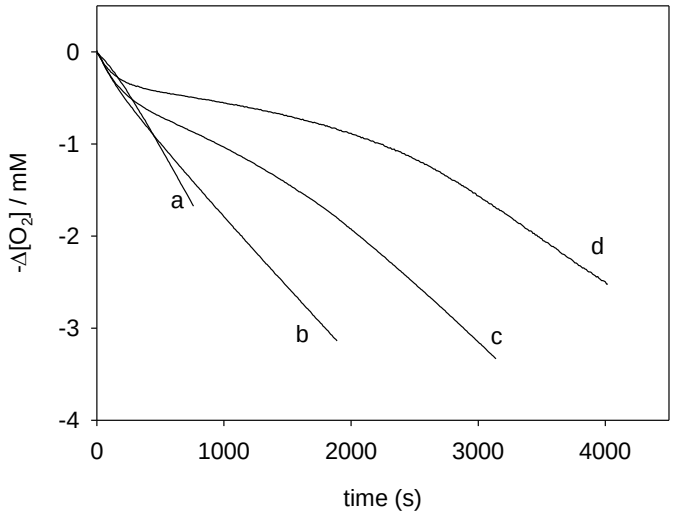

Figure S1. Oxygen consumption recorded during the autoxidation of styrene (4.3 M) in PhCl initiated by AIBN (0.05 M) at 303 K without inhibitors (a) and in the presence of: b) **5** (12 μM), c) **4** (6 mM), d) **6** (6.2 μM).

Calculations

DFT calculations were carried out using the Gaussian03 system of programs. Geometries and energies were computed at the B3LYP/6-31+G(d,p) level and the nature of the ground states were verified by frequency calculations (zero imaginary frequency).

The O-H BDE was obtained from the isodesmic reaction: XH + PhO• → X• + PhOH as reported (for instance) in: M. Guerra, R. Amorati, G. F. Pedulli, *J. Org. Chem.* **2004**, *69*, 5460-5467.

The enthalpies of the involved species were computed from frequency calculations at the B3LYP/6-31+g(d,p) level) in the gas phase and were scaled by a factor of 0.9806 to account for anharmonicity (A. P. Scott, L. Radom, *J. Phys. Chem.* **1996**, *100*, 16502–16513).

The standard **redox potentials** in MeCN (vs. NHE) were obtained from the experimental *E*° of α-tocopherol (α-TOH) and the isodesmic reaction:

$X^{red} + \alpha\text{-TOH}^{\bullet+} \rightarrow X^{ox} + \alpha\text{-TOH}$

The energies of the species involved were estimated by using the implicit solvation model (PCM) as implemented in Gaussian 03 (Total free energy in solution with all non electrostatic terms). In the case of those OH groups exposed to the solvent and not involved in intramolecular H-bonds, an explicit HCN molecule was used to simulate MeCN *as H-bond acceptor*, as shown in Figure S2. To reduce the calculation time, the piperidine in **4-6** was simplified to two methyl groups (see Figure S2).

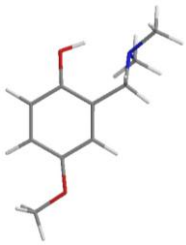

5 (parent phenol)

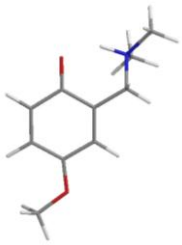

5 (radical cation)

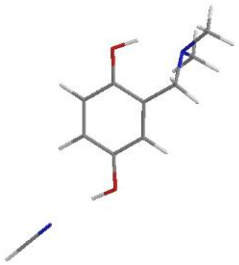

6 (parent phenol)

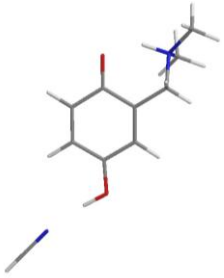

6 (radical cation)

Figure S2. Optimized structures for some investigated compounds.

In the Table S1, results obtained in the case of the H-bond formation between *para*-methoxyphenol, its radical cation and MeCN or HCN are reported. From this Table it can be inferred that the H-bond accepting ability of HCN is somewhat weaker than that of MeCN, as the OH---N distances for MeCN are shorter than those for HCN. The angles formed between the O-H and the N atoms of MeCN and HCN are instead very similar.

However, when considering the energies (see Table 1), the difference is very small, that is 0.000967 a.u. = 0.61 kcal/mol. This, in turn, corresponds to an overestimation of the redox potentials by 0.026 V, when using HCN instead of MeCN.

We believe that this small difference is acceptable, as it is comparable to the errors of the experimental determinations of redox potentials (for instance, E° for tocopherols are given with an error of ± 0.05 V). Our isodesmic approach is expected to lead to error cancellation, in particular those derived form using a medium-sized basis set, and from neglecting the basis set superimposition errors and the thermochemical correction.

Table S1. Results from geometry optimizations of the complexes between para-methoxyphenol and MeCN or HCN, and the subsequent SCRF calculations.

	H---N distance (Å)	O-H---N angle (°)	Total free energy in solution (a.u.)	Total free energy in solution difference (a.u.)
4-OMePhOH---NCMe	2.009	173	-554.789835	
4-OMePhOH$^{\bullet+}$---NCMe	1.649	174	-554.592379	
				0.197456
4-OMePhOH---NCH	2.070	171	-515.457828	
4-OMePhOH$^{\bullet+}$---NCH	1.731	173	-515.259405	
				0.198423

To further test the reliability of this method, besides compounds **1**-**7** reported in the main article, we calculated the *E*° for other structurally related molecules. Results, reported in Table S2, show that the calculated potentials are equal, within experimental error, to reference ones.

Table S2. Calculated and experimental redox potentials for phenolic antioxidant and a related molecule lacking the OH group.

reduced	oxidized	$E°_{calc}$ / V (vs. NHE)	$E°_{exp}$ / V (vs. NHE)
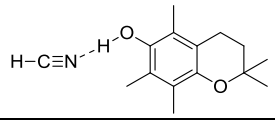	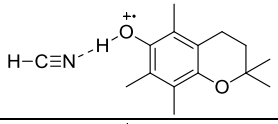	-	1.13±0.05
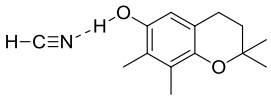	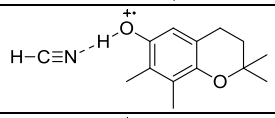	1.19	1.18±0.05
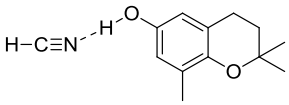	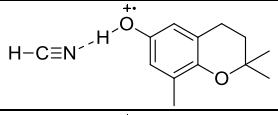	1.24	1.28±0.05
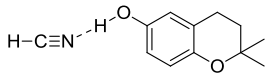	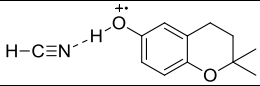	1.34	1.38±0.05
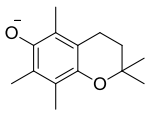	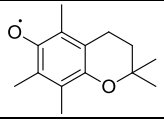	–0.30	–0.27±0.05
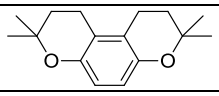	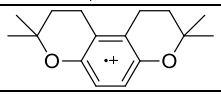	1.27	1.24±0.05[a]

a) from : H. M. Peng, B. F. Choules, W. W. Yao, Z. Zhang, R. D. Webster, P. M. W. Gill *J. Phys. Chem. B* **2008**, *112*, 10367–10374; L. L. Williams, R. D. Webster *J. Am. Chem. Soc.* **2004**, *126*, 12441-12450.

Calculation of the acidity of the radical cations from phenols 5 and 6.

Values of OH *BDE*, *E*° e pK_a in MeCN are related by the following thermodynamic cycle, taken from the recent review by Warren, Tronic and Mayer (ref 3).

BDE_{sol} = 1.37 pK_a + 23.06 *E*° + C_H

In the case of MeCN as solvent, C_H = 59.4 kcal/mol, if the reference electrode is ferrocene (Fc^+/Fc) (see Table 1 on pg. 6965, ref 3). The *E*° vs. (Fc^+/Fc) for the relevant redox couples was calculated by subtracting 0.630 V to *E*° vs. HNE (ref 12b).

The *BDE* values in MeCN were estimated by assuming that H-bond formation between the phenolic OH and MeCN increases the OH *BDE* by about 1.5 kcal mol^{-1}. In the case of **5**, this correction was not made because in this phenol there is only one OH group, which is already intramolecularly H-bonded and thus it doesn't form strong interactions with MeCN. The thermodynamic cycles and the pKa are reported in Figure S3.

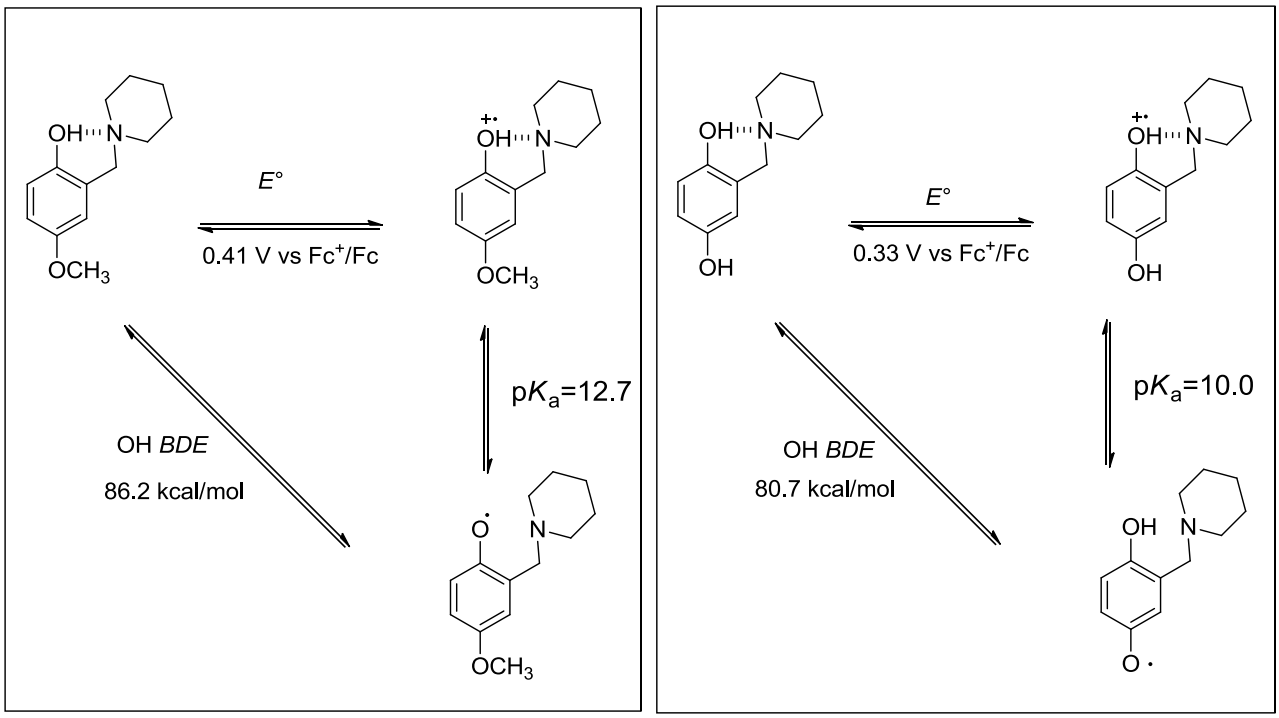
OH
N
OCH3
E°
0.41 V vs Fc+/Fc
+•
OH
N
OCH3
OH BDE
86.2 kcal/mol
pKa=12.7
O•
N
OCH3
OH
N
OH
E°
0.33 V vs Fc+/Fc
+•
OH
N
OH
OH BDE
80.7 kcal/mol
pKa=10.0
OH
N
O•

Figure S3.

Detail of dpph$^{\bullet}$ kinetics

The following Figures are representative examples of the kinetics of **4**, **5** and **6** with dpph$^{\bullet}$ in MeCN at 298 K.

5 + dpph$^{\bullet}$

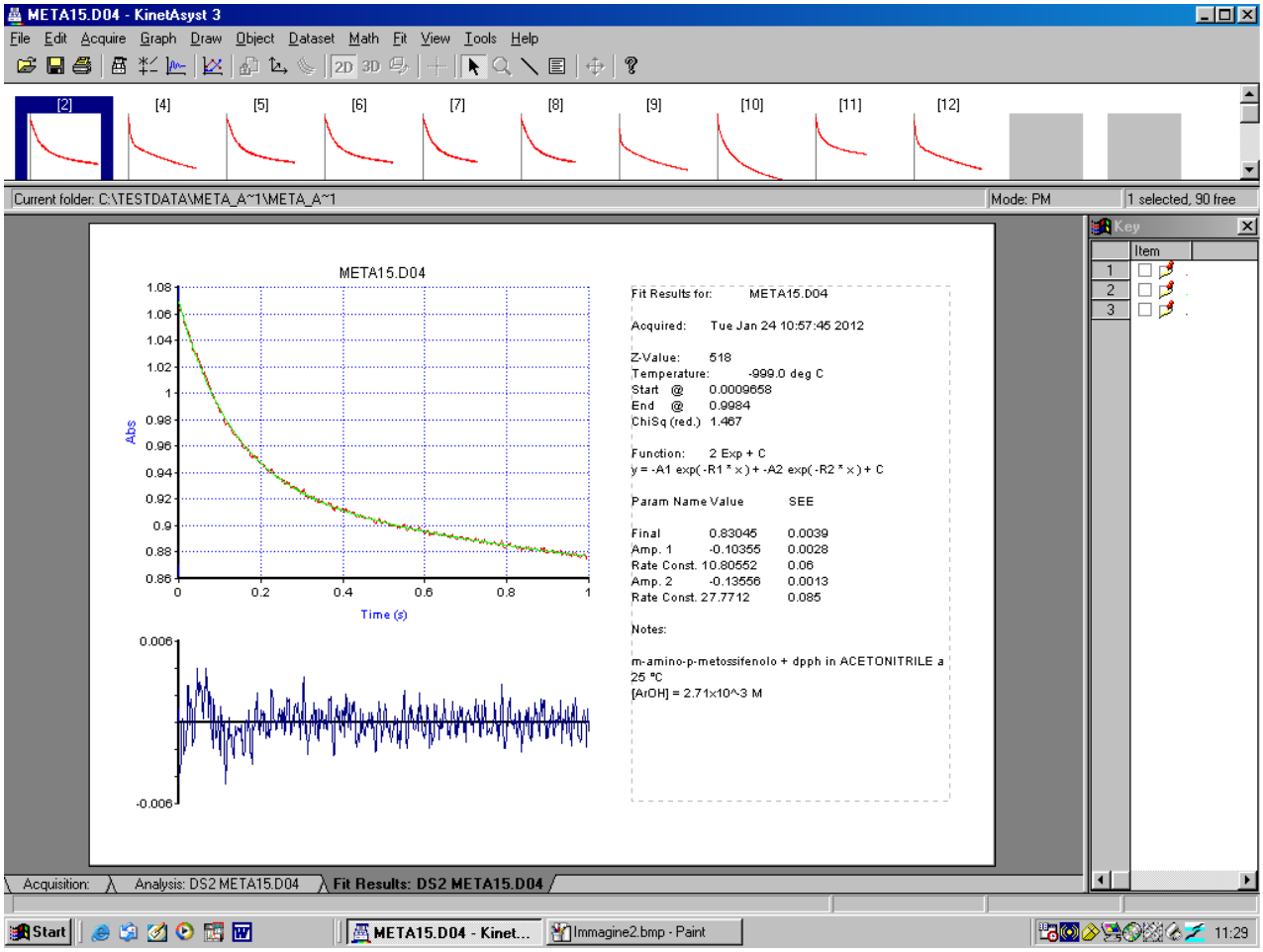

Figure S4. Phenol **5** (2.71×10^{-3} M) + dpph$^{\bullet}$ (9.6×10^{-5} M) in MeCN. The trace is fitted with a double exponential.

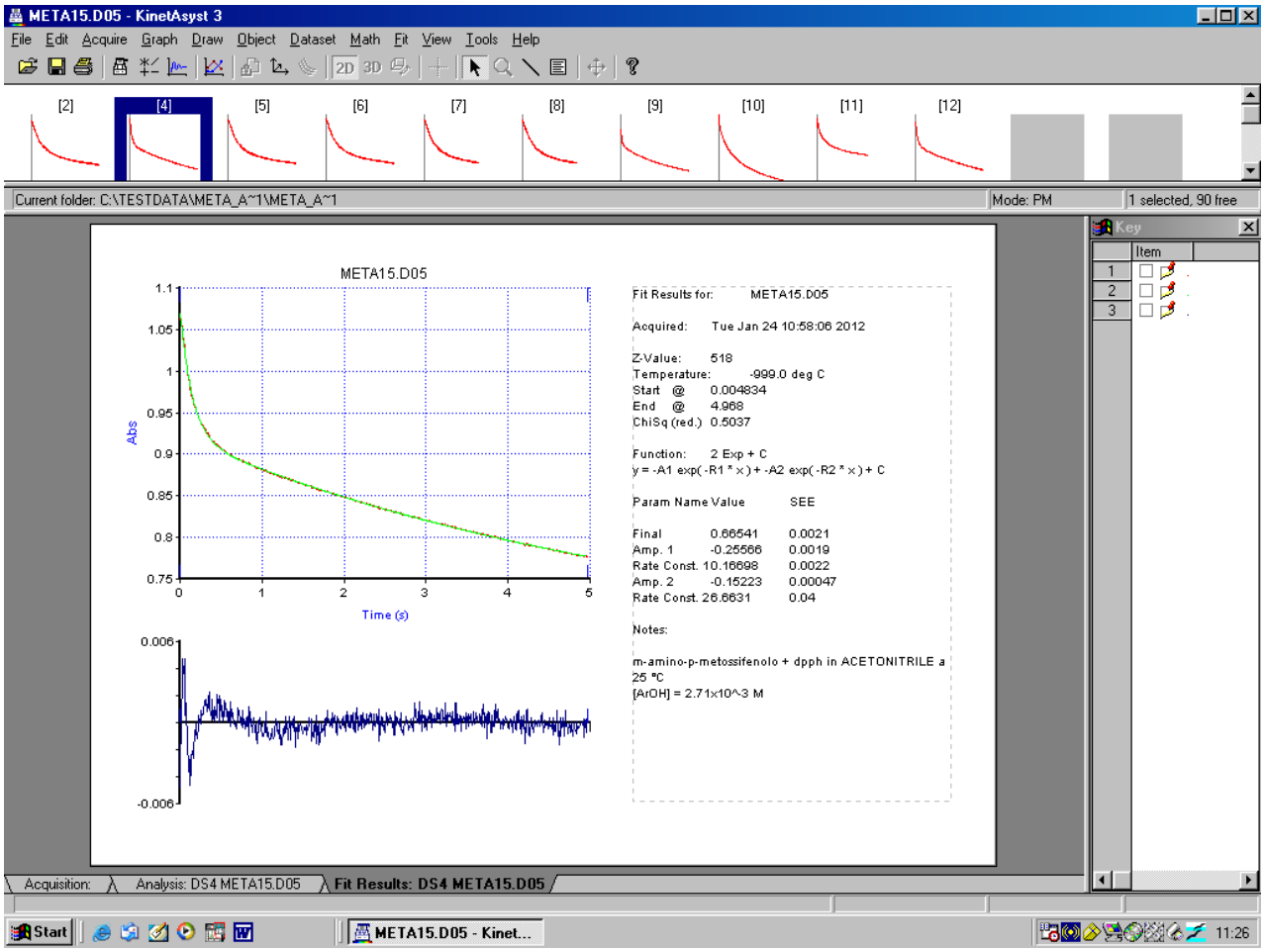

Figure S5. Phenol **5** (2.71×10^{-3} M) + dpph$^{\bullet}$ (9.6×10^{-5} M) in MeCN. The trace is fitted with a double exponential.

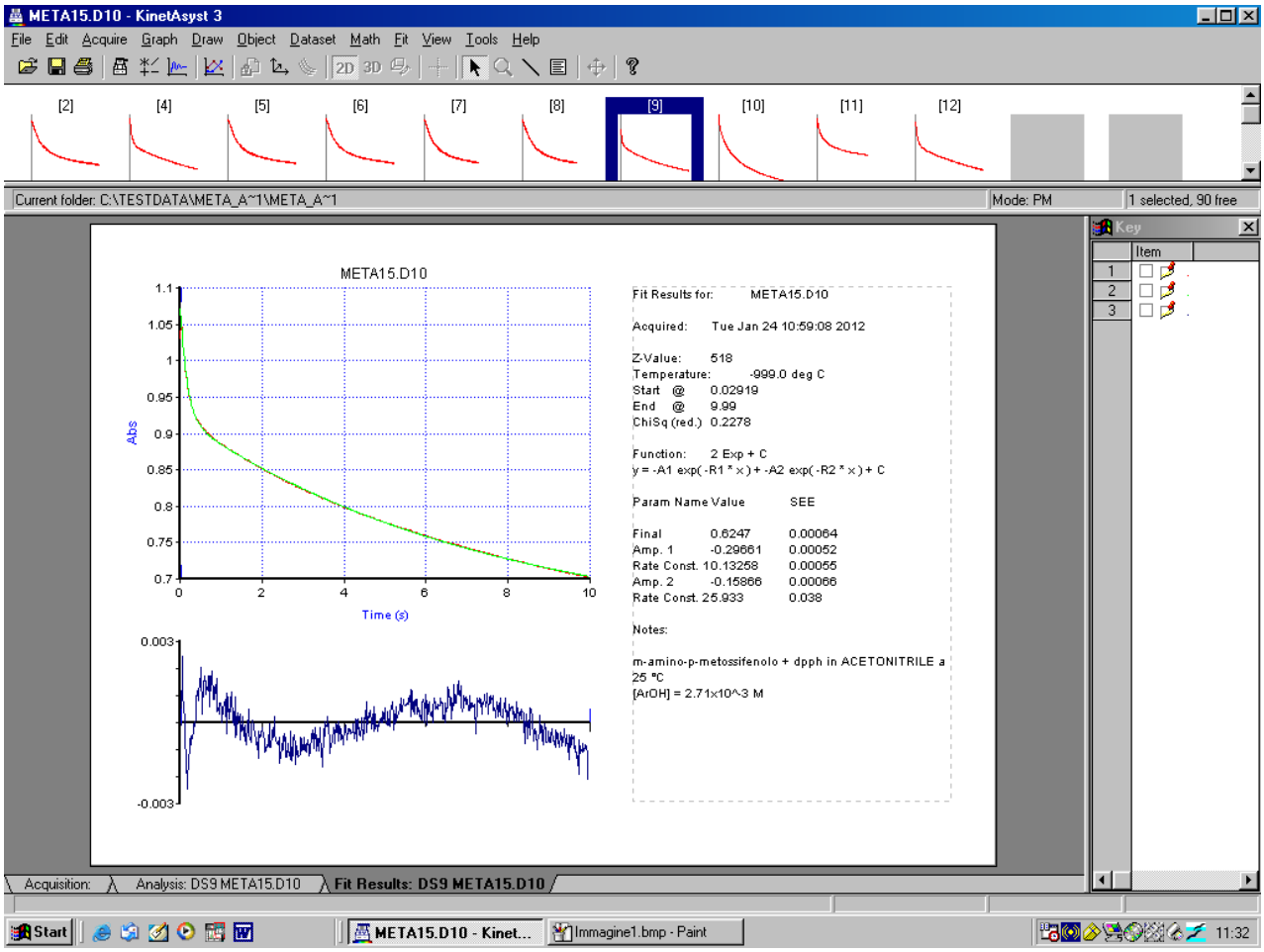

Figure S6. Phenol **5** (2.71×10^{-3} M) + dpph$^{\bullet}$ (9.6×10^{-5} M) in MeCN in a longer time scale. The trace is fitted with a double exponential. The residuals now show a pattern, though the variations are within -0.003 and 0.003. The rate constants are in fact pretty similar to those obtained above.

SIMULATIONS OF THE KINETICS OF 5 + dpph$^{\bullet}$ DONE WITH SPECFIT

The scheme of reaction is reported in the paper (Scheme 1) with the relevant rate constants.

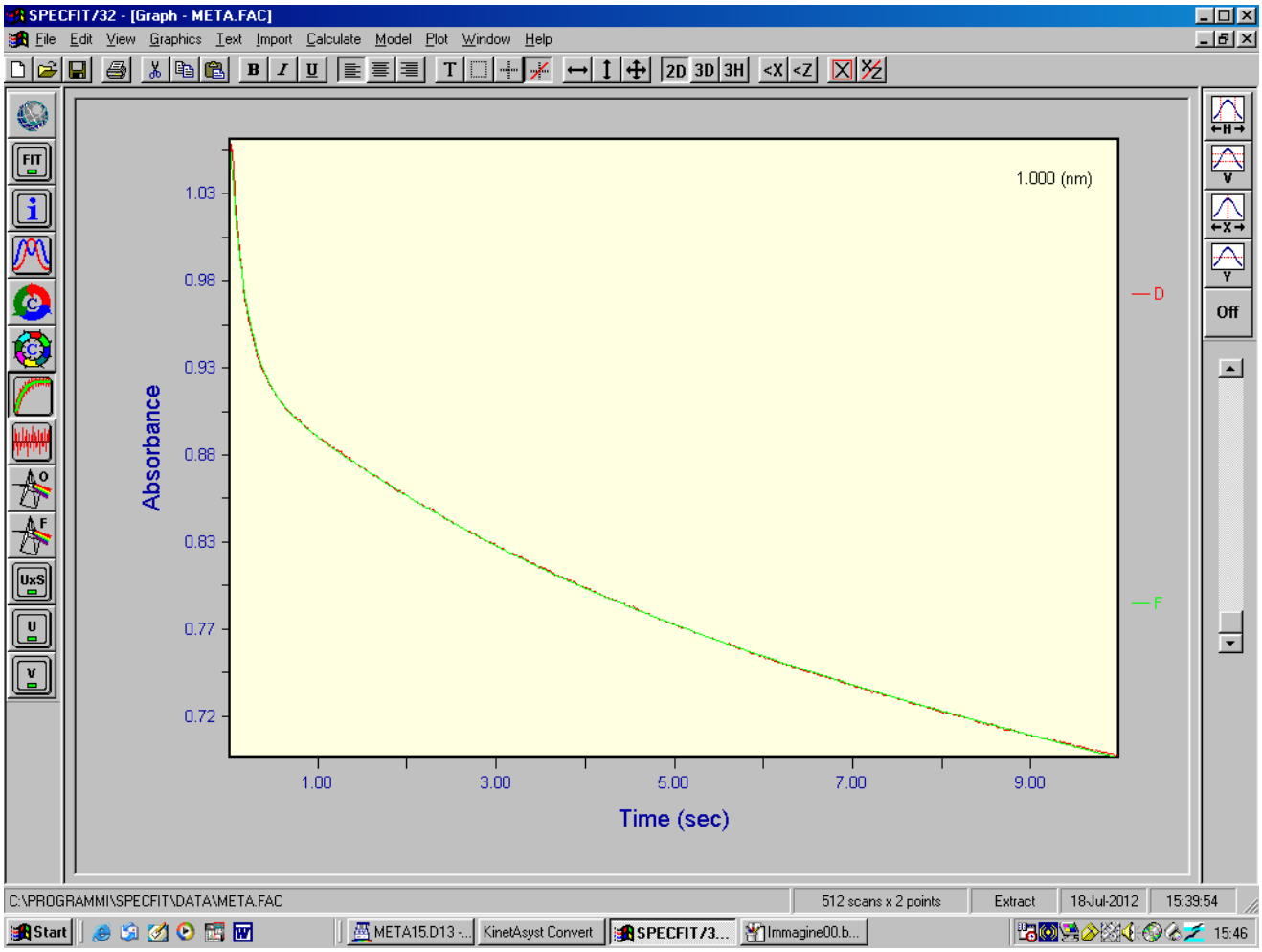

Figure S7. Simulation (green line) for **5** + dpph$^{\bullet}$ in acetonitrile at 298 K. The concentration of phenol was 2.71×10^{-3} M whereas that of dpph$^{\bullet}$ 9.6×10^{-5} M. The reaction scheme adopted in this simulation is that of Scheme 1 in the main paper.

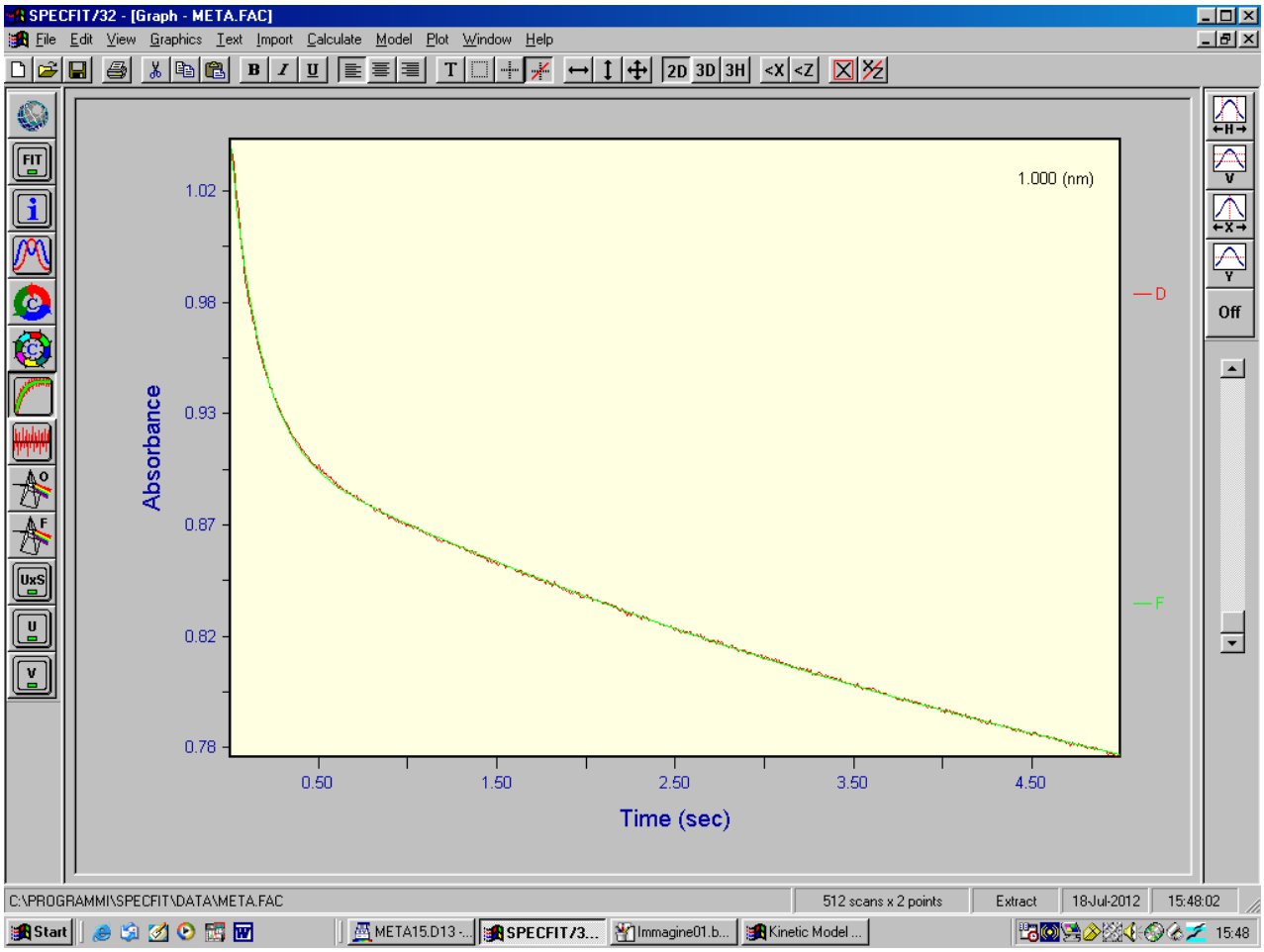

Figure S8. As above but in a shorter time scale.

6 + dpph

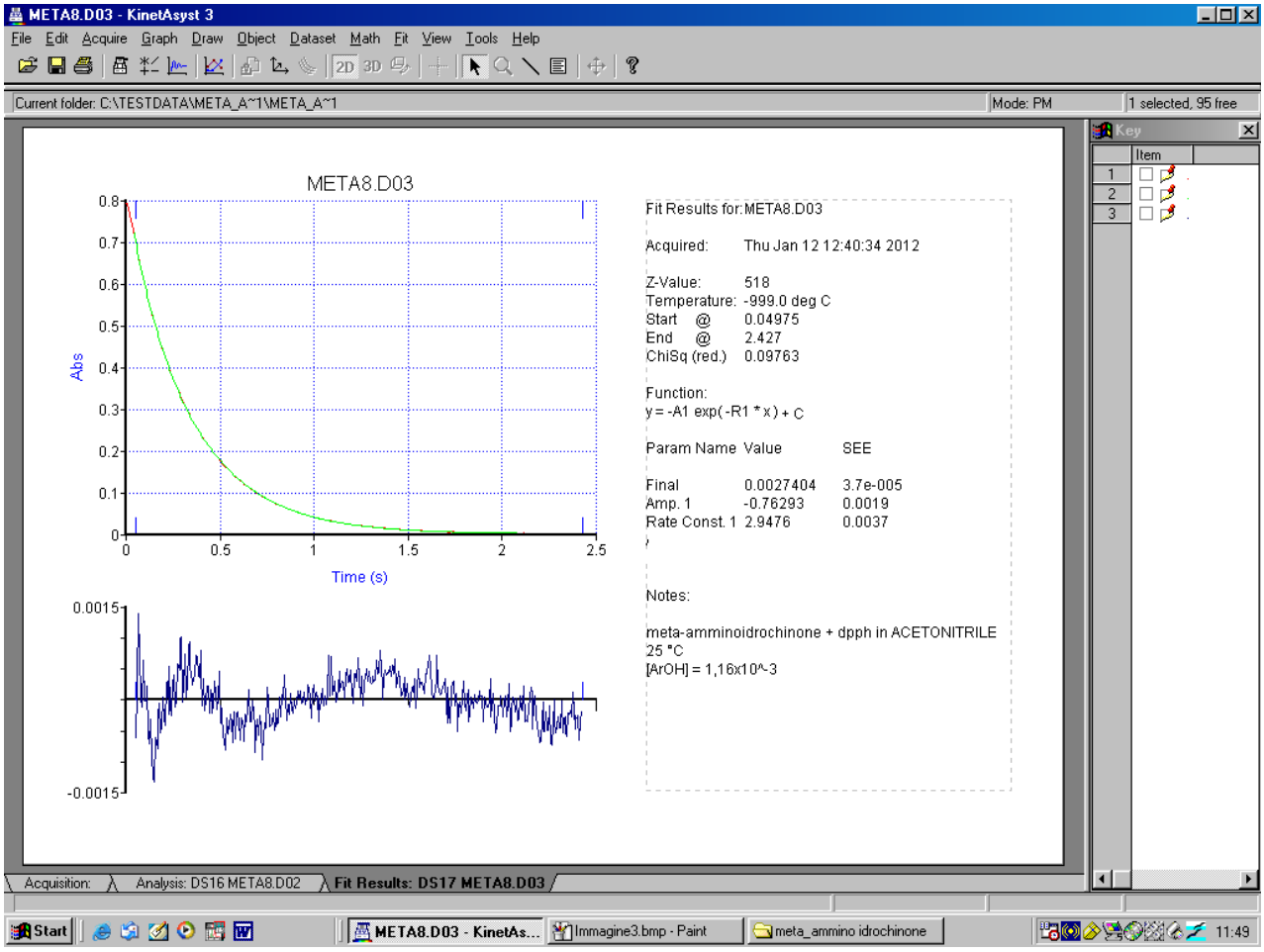

Figure S9. Phenol **6** (1.16×10^{-3} M) + dpph$^{\bullet}$ (7.3×10^{-5} M). The trace is fitted with a single exponential.

4 + dpph

The **4** + dpph reaction in acetonitrile is very interesting. The typical 518 nm bleaching following the addition of **4** to an acetonitrile solution of dpph$^{\bullet}$ is shown in Figure S10. The kinetics shows that the final absorbance of the mix – after complete consumption of dpph$^{\bullet}$ – is very high. Some visible-absorbing compound(s) must therefore be formed. We will show that this compound is simply the anion of dpph$^{\bullet}$, dpph^{-}, identified by spectroscopic evidence and formed by ET from the anion of **4** to dpph. The dpph^{-} anion is not usually observed in sequential proton-loss electron transfer (SPLET) reactions because it is readily neutralized by acids present in solutions. We have now the first example of SPLET in which the 'electron trap/sink' is 'exposed' in solution because phenol **4** and its ammonium ion are too weak acids to neutralize it.

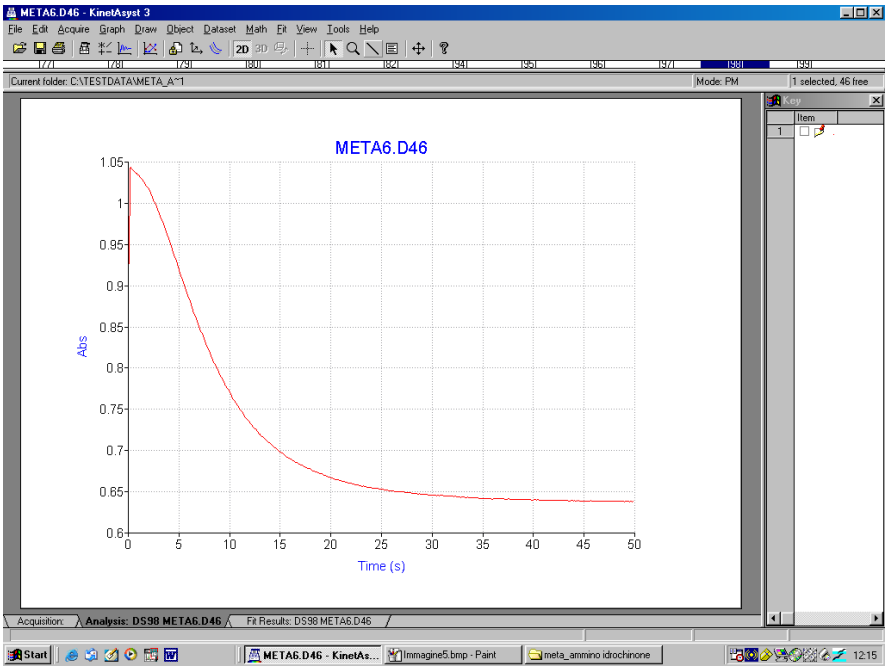

Figure S10. Decay of phenol **4** (7.8×10^{-4} M) + dpph$^{\bullet}$ (8.3×10^{-5} M) at 518 nm in acetonitrile at 298 K.

Along with the decay shown in Fig. 7 at λ = 518 nm (dpph$^{\bullet}$ λ_{max}), we observed a substantial build-up of the absorbance at 432 nm which is unusual in reactions with dpph$^{\bullet}$, see Fig. S11.

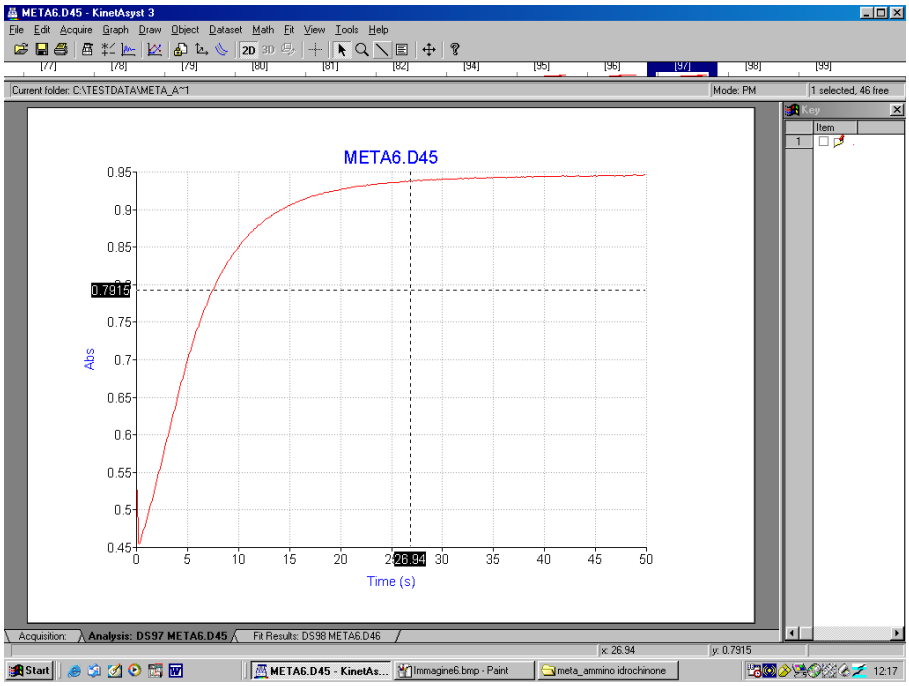

Figure S11. Phenol **4** (7.8×10^{-4} M) + dpph$^{\bullet}$ (8.3×10^{-5} M) at 432 nm in acetonitrile at 298 K.

Both the 518 nm decay and the 432 nm growth could be fitted (excluding the first 3 – 5 s of kinetics) with a mono-exponential function which essentially yielded the same rate constant, $k \approx 280 \pm 60$ $M^{-1}s^{-1}$ (see for an example Fig. 9). This large rate constant – not far from the value measured in cyclohexane ($k \approx 400 \pm 30$ $M^{-1}s^{-1}$) – excludes a hydrogen-atom transfer (HAT) mechanism since this in acetonitrile would be subjected to large KSEs (see phenol **7** in Table 1 in the paper). Therefore, the reaction demands an ET mechanism which is more properly identified as SPLET. Phenols are usually very weak acids in acetonitrile (pKa ≥ 27). However, phenol **4** has a strong pendant base and thus its auto-ionization may have an important role in the formation of the anion:

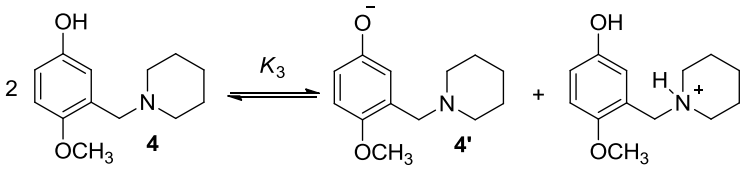

We estimate that the equilibrium constant of the above ionization is ~10^{-8} in acetonitrile at 298 K ($K_3 = K_a$ (**4**) / K_a (NH^+) = 10^{-27} / $10^{-18.8}$; NH^+ is the ammonium ion produced in the autoionization whose K_a should be very similar to that of Et_3NH^+, pK_a = 18.8). This equilibrium constant is large enough to produce significant concentrations of the phenol anion which reacts by ET with dpph,

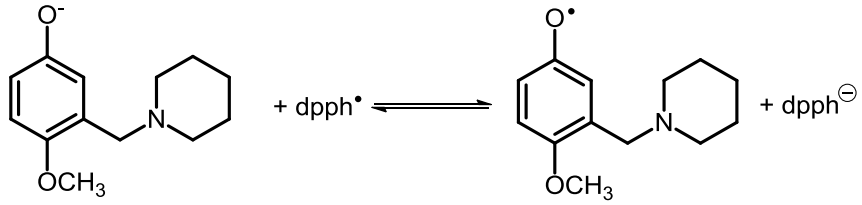

$$\Delta G^0 = -F\Delta E^0 = -F \times \left(E^0_{dpph} - E^0_{S'}\right) = -23.06\ (0.76 - 0.07) = -15.9\ \frac{\mathbf{kcal}}{\mathbf{mol}}$$

$$K_{eq} = \exp\left(-\frac{\Delta G^0}{RT}\right) = 5 \times 10^{11}$$

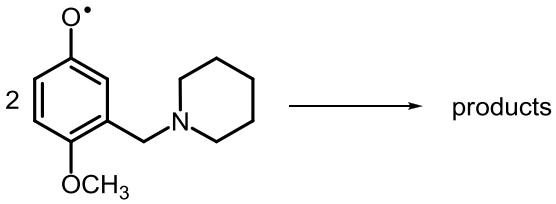

The observed rate constants were linearly dependent on the [**4**] within the range of phenol concentrations explored in our experiments (0.3 – 1.6 mM), see Fig. S12. Unfortunately, we could not use higher concentrations of **4** because of its poor solubility in acetonitrile. We suspect that the linear dependence shown in Fig. S12 is only a portion of a more complex dependence which as the

[**4**] is increased or decreased may determine a different reaction order in phenol (see ref. 6f and the SI therein).

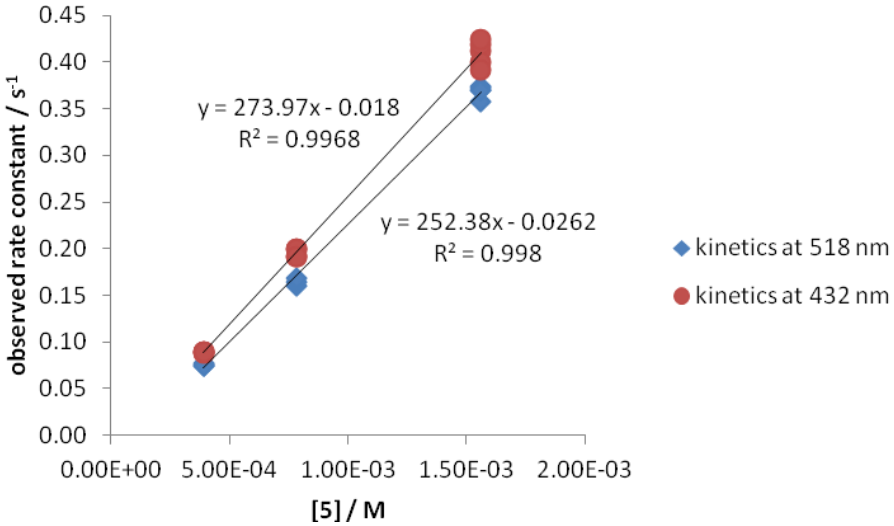

Figure S12. Observed rate constants for **4** + dpph$^{\bullet}$ in acetonitrile at 298 K determined at 518 nm and at 432 nm.

The spectrum of the final solution after complete consumption of dpph$^{\bullet}$ (t > 50 s, see Figs. S10 and S11) is given in Figure S13. It shows a stable and large absorption band with a max at about 432 nm.

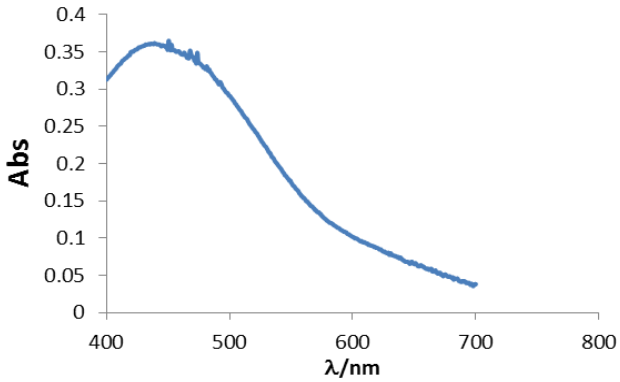

Figure S13. Final spectrum of **4** (7.8×10^{-4} M) + dpph$^{\bullet}$ (8.3×10^{-5} M) in acetonitrile at 298 K.

Since the final ET product according to our reaction mechanism must be the dpph^{-} anion we tried to produce it by treating an acetonitrile solution of dpphH with CH_3ONa but after the addition of the base we obtained only a brown precipitate (probably dpph^{-} Na^{+}) while the solution was colourless. However, the same treatment in MeOH yielded the dpph^{-} anion and the solution became (brown-) reddish. After rescaling for the different concentrations, the spectrum in Fig. S13 superimposed perfectly to that recorded in MeOH, see Figure S14. The small solvent effect

observed in the two spectra recorded in MeCN and MeOH is not surprising since also the spectra of the dpph radical differ very little in these two solvents. Therefore, we conclude that the spectrum recorded shortly after the reaction end, Fig. S13, is that of dpph$^-$.

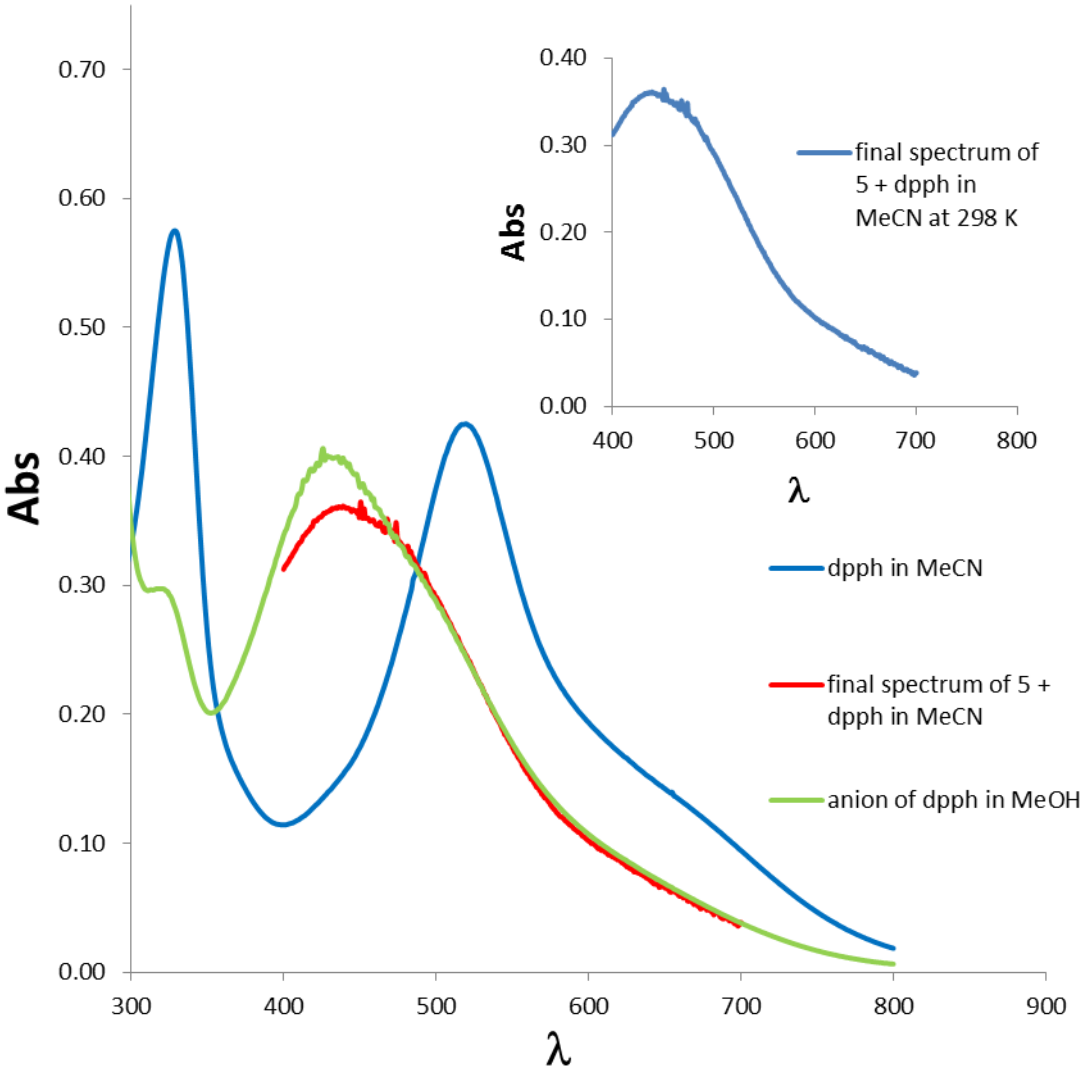

Figure S14. Spectra of dpph in MeCN, and of dpph$^-$ in MeCN and MeOH at room temperature.

Further experiments were performed to explore the mechanism of the reaction of **4** and dpph•. Addition of acetic acid reduced the reactivity of phenol **4** while addition of a N-base increased its reactivity. This is an additional proof that the reactive species is the anion of **4**.

Synthesis

General: Unless noted otherwise, materials were purchased from commercial suppliers and used without further purification. Pyridine was dried following standard procedures. Progress of reactions was monitored by thin-layer chromatography (TLC) on commercially available precoated plates (silica gel 60 F254) and the products were visualized with acid vanillin solution. Purification of the products was performed by flash column chromatography using silica gel 60 (230–400 mesh). Melting points were determined in a capillary tube using a Büchi 510 melting point apparatus. ^{1}H and ^{13}C NMR spectra were recorded at 400 or 200 and 100 or 50 MHz, respectively. Chemical shifts (δ) are expressed in ppm using residual non-deuterated solvent as an internal standard. Coupling constants (J) are given in Hertz (Hz). Mass spectra were obtained with a Shimadzu QP5050.

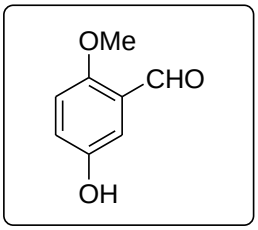

5-Hydroxy-2-methoxybenzaldehyde.[1,2] A solution of 2,5-dihydroxybenzaldehyde (1380 mg, 10.0 mmol) in anhydrous DMF (20 mL) was treated with K_2CO_3 (1380 mg, 10.0 mmol) at 25 °C, and the mixture was stirred for 30min. Methyl iodide (1850 mg, 13.0 mmol) was added, and the reaction mixture was further stirred for 20h before being quenched by the addition of H_2O (100 mL). The aqueous layer was extracted with Et_2O (2x100 mL). The combined organic layer was dried over Na_2SO_4 and concentrated under vacuum. The product was isolated by flash chromatography on silica gel (eluent cyclohexane:EtOAc/3:1) as a yellow solid (m.p. 112-115 °C, 47% yields). ^{1}H NMR (200 MHz, CD_3Cl_3) δ 3.88 (s, 3H), 6.03 (bs, OH), 6.90 (d, J = 9.0 Hz, 1H), 7.13 (dd, J = 9.0 and 3.3 Hz, 1H), 7.37 (d, J = 3.3 Hz, 1H), 10.40 (s, 1H, CHO) ppm; ^{13}C NMR (50 MHz, $CDCl_3$) δ 56.1 (1C), 113.4 (1C), 113.7 (1C), 123.8 (1C), 125.0 (1C), 149.9 (1C), 156.7 (1C), 190.4 (1C) ppm. Anal. Calcd. for $C_8H_8O_3$: C, 63.15; H, 5.30. Found: C, 63.60; H, 8.53; N, 5.46.

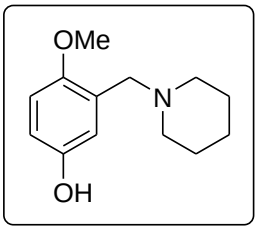

4-methoxy-3-(piperidin-1-ylmethyl)phenol (4). To a stirred solution of 5-hydroxy-2-methoxybenzaldehyde (465 mg, 3.00 mmol) and piperidine (1020 mg, 12.0 mmol) in methanol (8 mL) a solution of sodium cyanoborohydride (190 mg, 3.0 mmol) and zinc chloride (210 mg, 1.5 mmol) in methanol (5 mL) was added at room temperature. The resulting solution was stirred at room temperature for 2h and then taken up in 0.1N NaOH (50 mL). After most of methanol was evaporated under reduced pressure, the aqueous solution was

extracted with ethyl acetate (3x50 mL). The combined organic phases were washed with water and brine, dried over Na_2SO_4 and evaporated to dryness. The crude product was dissolved in ether and treated with HCl 1N to give the HCl salt, the aqueous layer was basified to PH >10 with NaOH and extracted with ethyl acetate to give the product as a beige solid (m.p. 140-142 °C, 60% yield). ^{1}H-NMR (400 MHz, CD_3OD) δ 1.40-1.46 (m, 2H), 1.56-1.61 (m, 4H), 2.46 (bs, 4H), 3.48 (s, 2H), 3.73 (s, 3H), 4.86 (s, OH), 6.67 (dd, *J* = 8.6 and 2.8 Hz, 1H), 6.77 (d, *J* = 2.8 Hz, 1H), 6.79 (d, *J* = 8.6 Hz, 1H) ppm; ^{13}C-NMR (100 MHz, CD_3OD) δ 25.1 (1C), 26.4 (2C), 55.2, (1C), 56.4 (1C), 57.6 (2C), 112.9 (1C), 115.7 (1C), 119.5 (1C), 126.8 (1C), 151.8 (1C), 153.0 (1C) ppm. MS: *m/z* (rel. int. %) 221 (M·+, 47), 190 (9), 137 (78), 98 (38), 84 (100); Anal. Calcd. for $C_{13}H_{19}NO_2$: C, 70.56; H, 8.65; N, 6.33. Found: C, 70.70; H, 8.53; N, 6.27.

Base pendant phenols 5 and 6 - General procedure[3]

To a solution of paraformaldehyde (600 mg, 20.0 mmol) in methanol (3 mL) of kept at 10 °C and containing approximately 2.5 mg of sodium hydroxide, a solution of piperidine (1700 mg. 20.0 mmol) in methanol (1 mL) of was added dropwise under stirring. Hydroquinone or 4-methoxyphenol (20.0 mmol) was added and the resulting solution was kept at reflux for 24 h hours. The crude mixture was diluted with EtOAc (100 mL) washed with a saturated solution of NH_4Cl (100 mL) and H_2O (3x100 mL). The organic layer was dried over anhydrous Na_2SO_4, concentrated *in vacuum* and purified by flash chromatography on silica gel.

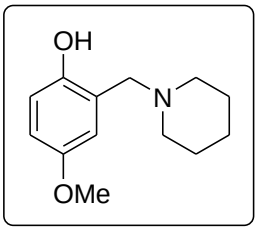

4-methoxy-2-(piperidin-1-ylmethyl)phenol (5). The product was obtained by flash chromatography on silica gel (eluent EtOAc) as colourless oil (50% yield). ^{1}H-NMR (400 MHz, $CDCl_3$) δ 1.48 (bs, 2H), 1.59-1.65 (m, 4H), 2.48 (bs, 4H), 3.61 (s, 2H), 3.73 (s, 3H), 6.53-6.54 (m, 1H), 6.69-6.75 (m, 2H) ppm; ^{13}C-NMR (100 MHz, CD_3Cl_3) δ 23.9 (1C), 25.8 (2C), 53.9, (1C), 55.7 (1C), 62.2 (2C), 113.2 (1C), 114.3 (1C), 116.2 (1C), 122.3 (1C), 151.8 (1C), 152.3 (1C) ppm. MS: *m/z* (rel. int. %) 221 (M·+, 68), 206 (14), 136 (26), 98 (16), 84 (100); Anal. Calcd. for $C_{13}H_{19}NO_2$: C, 70.56; H, 8.65; N, 6.33. Found: C, 70.83; H, 8.77; N, 6.41.

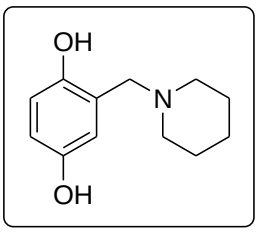

2-(piperidin-1-ylmethyl)benzene-1,4-diol (6). The product was obtained by flash chromatography on silica gel (eluent EtOAc) as a solid (m.p. 139 °C-dec., 40% yield). ^{1}H-NMR (400 MHz, $CDCl_3$) δ 1.49 (bs, 2H),

1.60-1.65 (m, 4H), 2.49 (bs, 4H), 3.59 (s, 2H), 6.50 (d, *J* = 2.8 Hz, 1H), 6.63 (dd, *J* = 8.6 and 2.8 Hz, 1H), 6.68 (d, *J* = 8.6 Hz, 1H), 7.16 (bs, 1H, OH) ppm; ^{13}C-NMR (100 MHz, $CDCl_3$) δ 23.9 (1C), 25.8 (2C), 53.8 (2C), 61.9 (1C), 115.1 (1C), 115.5 (1C), 116.4 (1C), 122.3 (1C), 148.2 (1C), 151.5 (1C) ppm. MS: *m/z* (rel. int. %) 207 (M·+, 27), 123 (9), 84 (100); Anal. Calcd. for $C_{12}H_{17}NO_2$: C, 69.54; H, 8.27; N, 6.76. Found: C, 69.25; H, 8.23; N, 6.71.

References

1. Boger, D. L.; Hong, J.; Hikota, M.; Ishida, M. *J. Am. Chem. Soc.* **1999**, *121*, 2471-2477.
2. Yang, H.; Li, Y.; Jiang, M.; Wang, J.; Fu, H. *Chem. Eur. J.* **2011**, *17*, 5652-5660.
3. Weatherbee, C.; Temple, R.; Burke, W.J. *J. Org. Chem.* **1956**, *21*, 1138-1141.